NLTE modeling of Fe II and [Fe II] lines in the shocked atmospheres of M Miras

He. Richter, P.R. Wood[1] , P. Woitke, U. Bolick and E. Sedlmayr

(Zentrum für Astronomie und Astrophysik, TU Berlin, D-10623 Berlin, Germany)
([1]Research School of Astronomy and Astrophysics, Australian National University, ACT 2611, Australia)

Correspondence to: richter@astro.physik.tu-berlin.de

1. Introduction

Our observations of cool, shock penetrated, expanding atmospheres of M-type Mira stars (see Richter & Wood 2001, A&A 369, 1027) showed that in particular the emission lines of Fe II and [Fe II] are good diagnostic tools to study the physical conditions in the shocked region close to the photosphere of these stars. The erratic appearance of these particular emission lines in stars which had just had a bright light maximum suggests that they require an exceptionally bright maximum for excitation. Presumably, these are associated with stronger shock waves caused by the stellar pulsation. According to the phase of their appearance it can be estimated, that the Fe II as well as the [Fe II] emission lines must originate close to the star at $\sim 1.5-3R_*$.

To model the Fe II and [Fe II] emission lines and to analyze the hydrodynamical conditions which lead to their formation, detailed NLTE radiative transfer calculations in spherical symmetry, applying a co-moving frame formalism and using accelerated lambda iteration have been carried out on a series of specific hydrodynamical shock structures. Our basic parameter studies reveal that the lines from ionized iron originate from hot post-shock zones and that they are in fact emitted close to the star's photosphere.

Dust formation takes place approximately in the same regions were the Fe II and [Fe II] emission lines originate from. Hence, a detailed study of these lines will offer the unique possibility to determine the physical conditions in the dust formation zone and thereby will shed some light on the basic mechanism of dust formation in M-type Mira stars.

2. NLTE Radiative transfer

The testing of the code as well as its application to model various CO absorption lines is presented on our poster contribution *U. Bolick* et al. "*NLTE modeling of lines in expanding shells of LPVs*". The following only gives a brief description of the code:

- **Radiative transfer:** time-independent, spherical symmetric, co-moving frame (CMF) (Mihalas et al. 1975).
- **Numerical approach:** Feautrier method, 2nd & 1st order discretisation (Richtmyer & Morton 1967).
- **Rate equation-system:** solved with gauss-solver and adjusted, damped newton iteration.
- **NLTE iteration:** by accelerated lambda operator (ALO) (Puls 1991; Rybicki & Hummer 1991).
- **FeII-model-atom:** 3-level-test-atom including one permitted: M38, 4583.84 Å and one forbidden emission line: 6F, 4417.51 Å; data from CHIANTI database (Dere et al. 1997).
- **Input models:** detailed radial shock structures at fixed time t_0 (Fig. 3) including Fe II and electron densities (see Sec. 3).

3. Radial shock structures

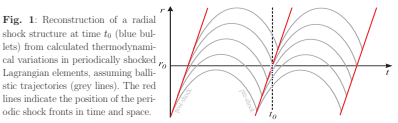

Fig. 1: Reconstruction of a radial shock structure at time t_0 (blue bullets) from calculated thermodynamical variations in periodically shocked Lagrangian elements, assuming ballistic trajectories (grey lines). The red lines indicate the position of the periodic shock fronts in time and space.

The radial shock structures used as input models for the radiative transfer calculations are obtained from thermodynamical gas-box models in the following way:

- **Simulation of the thermodynamical processes** in periodically shocked Lagrangian mass elements (Woitke et al. 1996b) by solving the energy equation $\frac{dh}{dt} = V\frac{dp}{dt} + Q_{\rm rad}$ between the shock transitions (h = specific enthalpy, V = specific volume, p = gas pressure, $Q_{\rm rad}$ = net radiative heating rate, P = pulsation period).
- **Classical Rankine Hugoniot relations** applied at every full period for the shock transitions, repeated until all thermodynamical variations have become periodical.
- **Detailed non-LTE gas model** to determine various particle densities, occupational numbers, $Q_{\rm rad}$ and the thermodynamic state functions in statistical equilibrium (described in Woitke et al. 1996a).
- **Iron ionisation** is treated in statistical equilibrium, taking into account photo-ionisation, direct recombination and collisional ionisation (including excited levels) on the basis of a 200-level Fe I and a 142-level Fe II model atom (Woitke&Sedlmayr 1999).
- **Continuous background radiation field** $J_\nu^{\rm cont}$ which enters into the various photo-rates. We assume a black body $J_\nu^{\rm cont} = B_\nu(T_{\rm rad})$ where $T_{\rm rad}$ is a radiation temperature chosen according to the stellar temperature and the radial distance r_0 of the shock front.
- **Optical depth effects** in spectral lines are described by the escape probability method (Sobolev theory). The mean velocity gradient is put to a fixed value of $\langle dv/dl\rangle = 10^{-7}\,{\rm s}^{-1}$.
- **Finally: Reconstruction of radial shock structures** $v(r)$, $\rho(r)$, $T(r)$, $n_{\rm FeII}(r)$, $n_{\rm el}(r)$ from the calculated temporal variations in the Lagrangian elements by assuming ballistic trajectories (see Fig. 1).

4. Observational constraints

Our observations (Richter & Wood 2001) showed that the permitted Fe II line M 38 and the forbidden line [Fe II] 6F (among other forbidden lines [Fe II] 7F, and [Fe II] 21F) belong to the faintest lines observed. They were detected at late phases around minimum visible light $\phi\sim 0.3$–0.5.

To estimate the region of emission we assume a pulsation period of 1 yr and a shock velocity of $v_{\rm sh} = 10\,{\rm km/s}$ ... $40\,{\rm km/s}$ which leads to a distance of $1...4\,R_*$ which the shock front travels in one period. With the assumption that the shock emerges from the photosphere (defined to be at optical depth one) at maximum $\phi = 0.0$, the radial position of the shock front R around minimum ($\phi = 0.5$) can be approximated to be $\sim R = 1.5...3\,R_*$. (This rough approximation neglects the shock deceleration on the way through the atmosphere). In summary one can conclude from the observations:

$\Longrightarrow$ Fe II emission lines should originate from a region of $\sim 1.5-3\ R_*$.

$\Longrightarrow$ Normalized peak fluxes $F_n = F_{\rm line}^{\rm peak}/F_{\rm cont}$ of these faint lines are in the limits $1.2 < F_n < 10$ (the lower limit being the detection limit).

5. Fe II & [Fe II] line fluxes

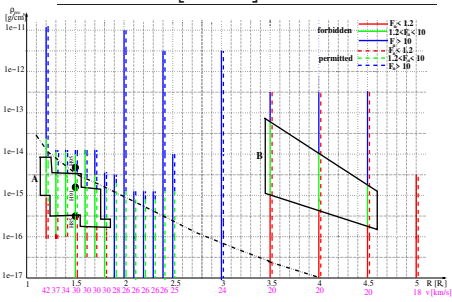

Fig. 2: Parameter study for the normalized peak line fluxes of the forbidden transition [Fe II] 6F (solid lines) and permitted transition Fe II M38 (dashed lines). The three varied parameters are: pre-shock density $\rho_{\rm pre}$, velocity amplitude of shock wave v and radial position of the shock front R. Results: Green lines mark calculated normalized peak fluxes in the observational limit, red lines mark fluxes lower and blue lines stand for fluxes bigger than the observed flux limit. For reference a radial pre-shock density structure from a hydrodynamical model of Schirrmacher et al. (2002) is given (dotted-dashed line). Bullets mark models shown in Fig. 3. Regions A and B see text.

To fit the observed normalized peak fluxes of the ionized iron lines in order to analyse from which atmospheric layers these lines are originating, parameter studies have been carried out: For a variety of fixed pairs of R and v the pre-shock density $\rho_{\rm pre}$ was varied and a gas-box model according to Sec. 3 was calculated. These radial structures were used as input models for the detailed NLTE radiative transfer calculations. The resulting normalized peak fluxes $F_n = F_{\rm line}^{\rm peak}/F_{\rm cont}$ were sorted into 3 categories: within in the observed limit $1.2 < F_n < 10$ (green lines), smaller than the detection limit $F_n < 1.2$ (red lines) or bigger than the observed limit $F_n > 10$ (blue lines) and accordingly marked in Fig. 2. We want to point out that the detailed line shapes are not of interest at this stage of our studies.

Fig. 2 depicts a parameter study up to 5 R_* with intermediate shock amplitude (additional parameter studies for $5-10\ R_*$ with $v < 18\,{\rm km/s}$ were resulting in too small normalized peak fluxes, so they are not depicted here). One can generally see that the normalized line fluxes of the forbidden and the permitted line are both within the observed limits close to the star $R = 1-2.5\,R_*$ whereas the normalized peak fluxes are much too small in the regions $R = 3.5-5\,R_*$. For models with $\rho_{\rm pre} > 10^{-14}$ g/cm^3 the normalized peak fluxes of the FeII-lines turn out to be too big. These pre-shock densities are bigger than the results from the hydrodynamical reference model of Schirrmacher et al. (2002) (dotted-dashed line in Fig. 2).

Two especially outstanding domains of Fig. 2 are discussed more detailed in the following:

• **Region B:** Fig. 2 shows that in region B at about $R = 3.5-4.5\,R_*$ the forbidden line fits the observed limits, but the permitted line is below the detection limit. As both lines where always observed in a pair this finding does not correspond to our observations. Also the pre-shock density in region B is too high according to our reference model ($\sim 1.5-3$ magnitudes higher).

• **Region A:** An astonishing result presented in Fig. 2 is that *only one* region exists, namely A, where the normalized peak flux of both calculated permitted and forbidden lines fit the observed fluxes. This region is close to the star's photosphere at $R = 1.2-1.8\,R_*$ and the densities therein correspond to our reference model in the upper limit, respectively being one order of magnitude lower for the lower limit of region A. Additionally region A fits the approximated position of the shock-front R around phase $\phi\sim 0.3$–0.5 (see also Sec. 4).

Examplary models around region A are plotted in Fig. 3. A detailed analysis shows that all gas-box models in region A have Fe II ion densities of $n_{\rm FeII} \sim 10^5...10^{5.5}\ 1/cm^3$ in the hot post-shock region. Higher ion densities generate too big whereas smaller ion density generate too small normalized peak fluxes in our radiative transfer calculations.

$\Longrightarrow$ We found that the Fe II density is the important limiting factor for the calculated normalized peak fluxes. This also leads to the conclusion that the Fe II emission lines can only originate from the hot post-shock region, where $n_{\rm FeII} \sim 10^5$ ... $10^{5.5}\ 1/cm^3$. The cooler post-shock regions do not contribute to the calculated fluxes.

• **Velocity amplitude variation:** Assuming the same pre-shock density we calculated models with varied velocity amplitudes in the shock wave in the intervall $1-2.1\,R_*$ (not depicted here) in order to study how region A changes. Our investigations show that a sufficiently high ion density of about $n_{\rm FeII} \sim 10^5$ ... $10^{5.5}\ 1/cm^3$ is reached at lower/higher pre-shock densities for models with higher/lower shock velocity amplitude. Consequently higher velocities shift region A towards lower densities and lower velocities cause a shift towards higher densities. No shift in the radial distance of region A is resulting.

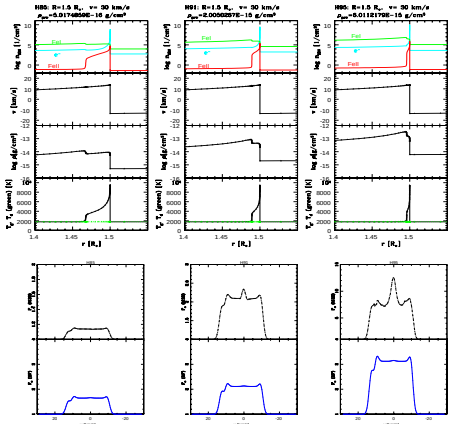

Fig. 3: *Upper row:* exemplary shock models as marked in Fig. 2 for $R = 1.5\,R_*$ (ordered from left to right by increasing pre-shock density): ion density $n_{\rm FeII}(r)$ of Fe II, Fe I and electrons; radial velocity $v(r)$; density $\rho(r)$; gas temperature $T_g(r)$ and black body temperature $T_R(r)$. *Lower row:* resulting NLTE line fluxes in units of normalized flux F_*: permitted M38 transition (upper panels), forbidden 6F transition (lower panels).

• **LTE/NLTE:** The analysis of the number densities in the levels and the transition rates yields (not depicted here) that in the hot post-shock region the upper level of the 6F transition ($E_u = 2.8$ eV) is in LTE, due to a dominance of collisional excitation, whereas the upper level of the M38 transition ($E_u = 5.5$ eV) is underpopulated with respect to the local thermodynamical equilibrium due to a dominance of spontaneous emission in the post-shock cooling gas.

6. Summary

Detailed NLTE radiative transfer calculations have been carried out on a series of specific shock structures in order to analyze the hydrodynamical conditions which lead to the formation of the observed Fe II and [Fe II] emission lines.

Our parameter studies reveal that there exists *only one* region close to the star's photosphere at $1.2-1.8\,R_*$ where both the normalized peak fluxes of the permitted and the forbidden line fit the observational limits. The pre-shock densities therein fit our reference model reasonably well and the radial position of this region corresponds to the region estimated from observations. The variation of region A according to different velocities amplitudes in the shock wave was investigated: higher/lower velocities lead to a formation of the right normalized peak fluxes at lower/higher pre-shock densities.

We conclude that the ion density of Fe II is the limiting factor for the calculated normalized peak fluxes and deduce that the Fe II emission lines can only originate from the hot post-shock region, where the Fe II density is sufficiently high, namely $n_{\rm FeII} \sim 10^5...10^{5.5}\ 1/cm^3$. We additionally note that the 6F line (4417.51 Å) is in LTE whereas the M38 line (4583.84 Å) is in NLTE.

Future work will have to provide detailed line profiles to fit the observed line shapes in order to extract the full information given by the Fe II and [Fe II] emission in M Miras. A detailed study of Fe II emission lines will reveal the physical conditions in the dust forming zones of M-type Mira stars, and nevertheless can be of general interest for the diagnostics of other astrophysical objects.

Acknowledgement:
We wish to thank Dr. J.M. Winters for his helpful advice and fruitful discussions. This work was supported by the *Deutscher Akademischer Austauschdienst, DAAD* with a HSP III grant, project number D/99/15656 and by the *Deutsche Forschungsgemeinschaft, DFG* project number SE 420/21-1, SE 420/21-2 and Sonderforschungsbereich 555, *Komplexe Nichtlineare Prozesse*, Teilprojekt B8.

References

Dere, K.P., Landi, E., Mason, H.E., Monsignori Fossi, B.C., Young, P.R.: 1997, A&AS **125**, 149
Mihalas, D., Kunasz, P.B., Hummer, D.G.: 1975, ApJ **202**, 465
Puls, J., Herrero A.: 1988, A&A **204**, 219
Puls, J.: 1991, A&A **248**, 581
Rybicki, G.B.: 1971, NBS Spec. Pub. **332**, 87
Rybicki, G.B., Hummer, D.G.: 1991, A&A **245**, 171
Richtmyer, R.D., Morton, K.W.: 1967, John Wiley & Sons, New York, 2nd edition
Richter, He., Wood, P.R.: 2001, A&A **369**, 1027
Schirrmacher, V., Woitke, P., Sedlmayr, E. : 2002, A&A in preparation
Woitke, P., Krueger, D., Sedlmayr, E.: 1996a, A&A **311**, 927
Woitke, P., Goeres, A., Sedlmayr, E.: 1996b, A&A **313**, 217
Woitke, P., Sedlmayr, E.: 1999, A&A **347**, 617

Grid (1 , 1)